How computed X-ray tomography can be used to study crosslink density in non-filled peroxide cured polyisoprene rubber

Sture Persson
SKEGA AB, S-934 02 Ersmark, Sweden
(Received 19 May 1987; revised 27 October 1987; accepted 4 November 1987)

As part of an ongoing research programme to investigate how medical X-ray computed tomography (CT) can be used in non-destructive testing of polymeric materials, a series of peroxide cured, non-filled polyisoprene rubbers with different crosslink densities were investigated. It was found that a normal medical X-ray CT scanner, thanks to its excellent contrast resolution, is capable of detecting density variations, caused by crosslinking, which exceed 2–3 mg cm^{-3}.

(Keywords: computed tomography; tomodensiometry; crosslink density; density; peroxide; polyisoprene rubber)

INTRODUCTION

Radiography is widely used as a non-destructive testing technique (NDT) in industry. Recently a new medical diagnostic technique, computed tomography (derived from the Greek word for slice, *tomos*) has been used to an increasing extent as an industrial method. Tomography, which is closely related to conventional radiography, has certain advantages over the latter. Radiography provides, at best, a somewhat distorted two-dimensional image of a three-dimensional object, whereas tomography provides a distortion-free two-dimensional image of a two-dimensional cross-section through an object. From a series of two-dimensional tomographs, a distortion-free three-dimensional image can be constructed.

Medical X-ray CT (computed tomography) sometimes also called CAT (computer assisted tomography) has been shown to be particularly suitable for the investigation of organic materials such as rubbers, plastics, wood, and a variety of other light materials including metals like aluminium and magnesium, since these materials have densities which do not differ much from that of human tissue. Tomodensiometry, i.e. the surveying of the densities in a thin slice arbitrarily 'cut' through the object under investigation, can successfully be performed with normal medical X-ray scanners since there is a linear relationship between the Hounsfield CT number[1,2] and the bulk density. Hospital X-ray CT scanners are well suited to investigate all materials built up from elements with an atomic number of 20 (Ca) or less, and with densities up to approximately 2 g cm^{-3} (ref. 3). Elements with an atomic number of less than 20 are those normally found in polymeric materials such as H, C, N, O, F, Si, P, S, Cl. Few polymeric materials have densities exceeding 2 g cm^{-3}.

Since tomographic images are reconstructed from X-ray intensity measurements that are subject to statistical variations, the reconstructed linear attenuation coefficient (μ) of the material under investigation will have an associated statistical variance σ_μ^2. The precision with which a given μ can be determined from a single picture element (pixel) in a tomographic image is determined by this standard deviation σ_μ. Typical standard deviations are 1–5% which, compared with normal radiography, represent an improvement in the contrast resolution of at least two orders of magnitude. A measuring technique that offers such detailed information non-invasively and non-destructively probably has as much to offer to industry as to medicine.

The Hounsfield unit

The linear attenuation coefficient (μ) in computed tomography is represented by the Hounsfield scale. The unit of this scale is H (Hounsfield) in honour of one of the two inventors. Just like Fahrenheit, who related his temperature scale to the temperature of the human body, Hounsfield related his new scale to his own scanner, the EMI mark I, which operated at 120 kV with an aluminium filter of 4.5 mm and a water box of 27 cm. Under these conditions, the μ value of water was found to be 0.19 cm^{-1}, which is equivalent to the μ value of water measured with a monochromatic beam of 73 keV. The Hounsfield unit or the CT number of a substance 'X' was therefore defined by the following equation:

$$CT_{number} = 1000\frac{\mu_X - \mu_{water\ at\ 73\,keV}}{\mu_{water\ at\ 73\,keV}}$$
$$= 5263\mu_X - 1000$$

From the above formula it can be calculated that the CT number of water is 0, whilst that of air is −1000 and that of dense bone is up to +3095 H. Thus a scanner system can assign 4096 different H values to each picture element.

The linear attenuation coefficient, beam hardening and reconstruction methods

As tomography is not yet very widely used in industrial NDT, let us recall some basic phenomena related to the attenuation of X-rays by matter. The local attenuation characteristic of different materials for X-rays is the product of a series of interactions between X-rays and

0032-3861/88/050802-06$03.00

matter such as photoelectric absorption and Compton scatter[4]. Together, these two processes can be described by the parameter μ which is defined as the ratio of the intensities of exiting and incident beams.

Photoelectric absorption is a phenomenon whereby an X-ray photon is completely absorbed by an atom. Some of the energy absorbed is used to eject an electron from the atom, the remainder of the energy being used to impart to the ejected electron kinetic energy which will later gradually be lost by successive collisions. Compton scatter is the interaction of an X-ray photon with an electron which results in the generation of a secondary X-ray photon of a lower energy than that of the impinging X-ray photon. Both these processes have a specific probability depending partly upon the type of matter transversed by the photon and partly upon the energy of the photon.

Different materials have properties that contribute in different ways to the attenuation of X-rays. The atomic number greatly influences the photoelectric adsorption whereas the electron density has a great influence on the Compton scatter. When a *monochromatic* X-ray penetrates *homogeneous* matter, the intensity of the exiting beam is described by the following formula:

$$I = I_0 e^{-(\mu_E d)} \tag{1}$$

where I = intensity of exiting beam, I_0 = intensity of incident beam, E = energy of incident beam, d = thickness of object and e = base of natural logarithm = 2.718.

Equation (1) can be solved for the product $\mu_E d$,

$$\ln(I_0/I) = \mu_E d \tag{2}$$

When the X-ray penetrates through non-homogeneous matter, the ray path can be considered to consist of a (large) number of elements of thickness, w, with attenuation coefficients $\mu_1, \mu_2, \mu_3, \ldots, \mu_n$ as shown in *Figure 1b* (ref. 5).

Equation (2) then becomes

$$\ln(I_0/I) = \mu_1 w + \mu_2 w + \mu_3 w + \cdots + \mu_n w \tag{3}$$

This means that the logarithm of the measured transmission along a particular X-ray is the sum of the attenuations of all the elements that the X-ray passes through. The quantity $\ln(I_0/I)$ is normally termed a ray sum[5].

Since the X-rays generated by normal X-ray tubes are not monochromatic but comprise a complete spectrum of energies, it is clear that μ is a complex function that can have different values according to the radiation circumstances, i.e. μ is an energy-dependent parameter. Consequently equation (3) is valid only if μ corresponds to the average of all energies present in the X-ray beam. The energy dependence of μ is such that μ is large for low energies and small for high energies, i.e. lower energies are filtered out more rapidly than higher energies in the X-ray spectrum. Consequently the effective μ of the material decreases as the X-ray beam traverses the object. This phenomenon is usually called beam hardening and careful calibration must be carried out to avoid inhomogeneities in CT images as a result of this effect.

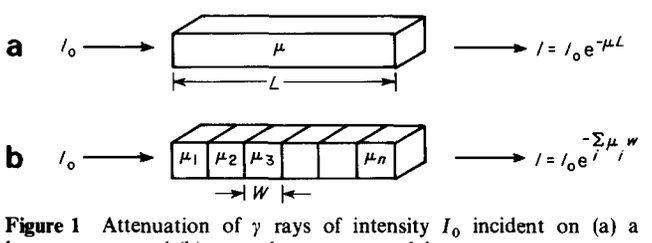

Figure 1 Attenuation of γ rays of intensity I_0 incident on (a) a homogeneous and (b) a non-homogeneous slab

In addition, if the object under investigation is not homogeneous, the magnitude of the beam hardening will be different at each projection during the scanning operation. In order to make it possible correctly to reconstruct an image, it is necessary to compute μ at each location within the slice, averaged over all beam energies passing through that location from different projections. Due to the large amount of data involved in the calculation of the linear attenuation coefficients, powerful computers are needed. The computer is also required to reconstruct the tomographic image from the measured ray sums. A large number of mathematical algorithms have been developed for the reconstruction of CT images, of which the most often used technique is called linear superposition of filtered back projections. This technique is described in detail in reference 6.

Dose and noise

If a homogeneous object is scanned, a water phantom for example, it is found that the CT numbers for a slice through the water do not all have the same value, as could be expected. The recorded CT numbers or attenuation values are randomly distributed around some average value.

The noise can be expressed as the standard deviation, σ_μ, of the attenuation coefficient, μ. The noise depends on the size of the object, on the X-ray tube voltage (kV_p), on the picture element (pixel) width, on the slice thickness and on the surface or skin dose. The relationship between noise and these parameters is expressed as follows[7]:

$$\sigma = k\left(\frac{B}{w^3 h D}\right)^{1/2} \tag{4}$$

where $B = e^{\mu d}$ and σ = standard deviation of the noise, k = machine-dependent constant, B = attenuation factor of the object, μ = linear attenuation coefficient, w = pixel width, h = slice thickness, D = maximum surface dose per slice and d = slice diameter.

From this formula it can be seen that the higher the dose the lower the noise: the dose must be increased by a factor of 4 in order to decrease the noise by a factor of 2.

Noise is a very important measure of the performance of a CT scanner since it limits the range of density differences that can be detected.

The standard deviation, σ, gives the precision with which a given μ can be determined from a single pixel in a tomographic image. The standard deviation is typically approximately 1–5%, which represents a contrast resolution at least two orders of magnitude better than normal radiography.

Contrast resolution

Contrast resolution, sometimes also referred to as density resolution, is the ability of a system to discriminate details of a certain size from their surrounding structures when these details have a low contrast relative to that of adjacent structures. In this definition it is assumed that the details to be detected are large enough for the system to detect them.

The following equation gives the percentage relative contrast:

$$\frac{100(a-b)}{a}\ \% \qquad (5)$$

where a and b represent the higher and the lower density values, respectively.

Spatial resolution

Spatial resolution is the ability of a system to distinguish small details from their background when these details have a sufficiently high contrast relative to that of adjacent structures for the system to be able to detect them.

It might generally be expected that the smallest object that could be detected would be equal to the pixel size. Practice has shown that the smallest discernible detail should have a size which is about 1.5 times larger than the pixel, preventing the pixel size from becoming a limiting factor. Pixel sizes for different CT scanners are shown in reference 2.

The slice thickness directly influences the spatial resolution. By varying the slice thickness the voxel (volume picture element) will be altered and the amount of averaging will therefore also be changed.

This short survey of the main parameters governing the image quality, indicates that conflicting situations may arise when an attempt is made to optimize image quality by setting all parameters to optimum conditions.

Generally, optimum image quality means high contrast resolution and high spatial resolution.

High *contrast* resolution requires:

High dose
Large pixel size
Thick slice

since these factors contribute to a high signal-to-noise ratio (eq. (4)). However, the pixel size cannot be too large or the slice too thick, otherwise the spatial resolution will be impaired.

High *spatial* resolution requires:

Small pixel size
Thin slice

A small pixel size and a thin slice will however cause an increase in the noise level and consequently a loss of contrast resolution. Moreover, decreasing the size of the pixel, or in other words increasing the number of pixels in a given matrix, calls for an increase in the number of measurements, which in turn increases the scan time and the image processing time.

EXPERIMENT I

The rubber compounds used are shown in *Table 1*.

Both the rubber and the peroxide were used as received and carefully mixed on a well cleaned 12 in laboratory two-roll mill. Test sheets with a thickness of 2 mm were press moulded at 140°C for 60 min. After cure all the test sheets showed a high degree of transparency with no sign of carbon black contamination.

Small samples were cut from the moulded test sheets and very carefully weighed in air and ethyl alcohol (ρ = 0.8086 at +20°C) using a microbalance. The bulk density was calculated according to the procedures described in reference 8. The results obtained (ρ_{HS}) are shown in *Table 1*.

The density gradient column was prepared according to instructions given in reference 9 and used in a thermostated room at $+23 \pm 0.1$°C.

The results obtained with the density gradient column (ρ_{DGC}) are also included in *Table 1*. From knowledge of

Table 1 Density data for experimental compounds

Ingredient	Chemical composition	Manufacturer and trade mark	Density ($g\,cm^{-3}$)	Parts by weight									
Synthetic natural rubber	*cis*-1,4 polyisoprene 92–99% *cis*-1,4 configuration	USSR origin SKI-3 NS	0.91	99	97	95	92	90	87	84	80	75	68
Peroxide	Dicumylperoxide 99% active (DCP)	Pennwalt. Luperox GmbH West-German Luperco 500R	1.001	1	3	5	8	10	13	16	20	25	32
Density ($g\,cm^{-3}$) Hydrostatic method (ρ_{HS})				0.9053	0.9130	0.9168	0.9236	0.9292	0.9339	0.9394	0.9490	0.9735	0.9812
Density gradient column (ρ_{DGC})						0.9122	0.9192	0.9248	0.9337	0.9387	0.9475	0.9695	
Calculated density ($\rho_{calc.}$) $\rho_{NR} = 0.9066$ $\rho_{perox.} = 1.001$				0.9075	0.9094	0.9113	0.9142	0.9160	0.9189	0.9217	0.9255	0.9302	0.9368
Apparent crosslink density ($mol\,cm^{-3} \times 10^{-4}$)				1.00	2.58	4.08	7.12	9.91	15.27	18.38	23.00	33.89	36.10
Standard deviation of apparent crosslink density (six measurements)				0.30	0.13	0.33	0.14	1.59	0.34	0.93	2.82	0.44	0.91

the weight fractions of polyisoprene and dicumyl peroxide (DCP) and their densities, the compound densities can be calculated. These calculated densities ($\rho_{calc.}$) are also shown in *Table 1*.

The apparent crosslink density was determined according to the procedure described in reference 10 using n-heptane as a solvent. The polymer–solvent interaction parameter (χ) used was 0.436 (ref. 11).

Results and discussion

The plot of bulk density (ρ_{HS} and ρ_{DGC}) against apparent crosslink density (ACD) in *Figure 2* shows the *combined* effect of the bulk density increase caused by:

(1) addition of increasing amounts of dicumyl peroxide to the polyisoprene rubber and

(2) the increase in crosslink density and hence being a result of a decrease in free volume of the molecular network[12].

The contributions of (1) and (2) to the total bulk density increase can be easily resolved simply by subtracting the calculated density ($\rho_{calc.}$), which corresponds to the density of the uncured compound, from the measured density of the cured compound, e.g. the hydrostatically determined values. Plots of measured bulk density (ρ_{HS}) and (ρ_{DGC}) against ACD (in mol $cm^{-3} \times 10^{-4}$) are shown in *Figure 2*. The density gradient column consistently gives somewhat lower values (ρ_{DGC}) than the hydrostatic method (ρ_{HS}) as shown in *Figure 2*. The reason for this is unknown.

The linear regression equation for ρ_{HS} vs. ACD is:

$$\rho_{HS} = 0.9066 + 0.001975\,ACD \qquad (6)$$

and the correlation coefficient, $r = 0.993$.

By using the extrapolated density (0.9066) at crosslink density 0, i.e. the density given by the intercept of the regression line with the y-axis, as a true value of the bulk density of pure polyisoprene rubber, the densities ($\rho_{calc.}$) shown in *Table 1* were calculated. They are also plotted as a function of ACD in *Figure 2*.

The linear regression equation for $\rho_{calc.}$ against ACD (mol $cm^{-3} \times 10^{-4}$) is

$$\rho_{calc.} = 0.9079 + 0.00074255\,ACD \qquad (7)$$

By subtracting the slope of the calculated density regression line from the slope of the measured density regression line, the regression line for $\rho_{crossl.}$ against ACD is obtained.

$$\rho_{crossl.} = 0.9066 + 0.0012325\,ACD \qquad (8)$$

The contribution of the crosslinking reaction to the density increase can then be easily obtained as follows.

Contribution of crosslinking to the density increase

$$= \frac{\text{slope of } \rho_{HS} - \text{slope of } \rho_{calc.}}{\text{slope of } \rho_{HS}}$$

$$= \frac{0.001975 - 0.00074255}{0.001975} = 0.624 \qquad (9)$$

Approximately 62% of the *density increase* originates therefore from the formation of crosslinks while the remaining 38% of the density increase is caused by the addition of the peroxide itself to the compounds. It is interesting to note that as much as 62% of the density increase is caused by the crosslinks, since this opens up the possibility of studying the crosslink density or the state of cure simply by measuring the increase in bulk density by any method sensitive enough to be able to detect small density variations. Computed X-ray tomography is ideally suited for this task since it has a very high contrast or density resolution.

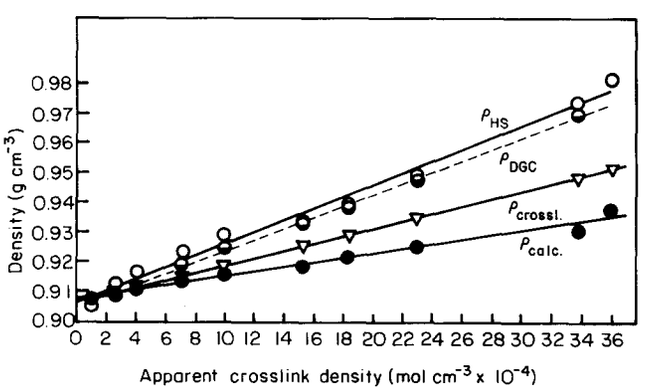

Figure 2 Density using hydrostatic (ρ_{HS}) and density gradient column methods (ρ_{DGC}) together with calculated density ($\rho_{calc.}$) and the contribution of crosslinking ($\rho_{crossl.}$) to the density increase as a function of apparent crosslink density for peroxide-cured synthetic *cis*-1,4 polyisoprene

EXPERIMENT II

In order to investigate the possibility of using CT to measure the small density increase caused by crosslinking, new compounds were mixed from the same materials as in Experiment I. The details of the compounds are shown in *Table 2*.

Test specimens to be used for the tomographic experiments were $70 \times 15 \times 110$ mm for compounds containing 3, 8 and 13% DCP and $70 \times (5 + 5) \times 110$ mm, i.e. two 5 mm rubber sheets firmly pressed together for compounds containing 16, 20 and 25% DCP. The rubber sheets were all cured for 60 min at +140°C.

Small samples were removed from the large specimen, some of which were used to measure the density using the density gradient column (ρ_{DGC}) and some were used to determine ACD according to the previously described procedure[9]. The results are shown in *Table 2*.

Results and discussion

The linear regression equation for ρ_{HS} against ACD in *Figure 2* is:

$$\rho_{HS} = 0.9080 + 0.0016145\,ACD \qquad (10)$$

$r = 0.992$.

The calculated densities ($\rho_{calc.}$) based on the intercept density for natural rubber in the equation (0.9080) are also shown in *Table 2*.

The linear regression equation for $\rho_{calc.}$ against ACD is:

$$\rho_{calc.} = 0.9109 + 0.0005342\,ACD \qquad (11)$$

$r = 0.985$.

By subtracting the slope of the calculated density $\rho_{calc.}$, i.e. the density of the uncured compounds, from the slope of the cured compounds, ρ_{HS}, we obtain the slope of the curve representing the contribution to the density increase given by the curing.

Table 2 Data for experimental compounds for CT measurements

Parts by weight SKI 3 NS	97	92	87	84	80	75
Parts by weight Luperco 500R	3	8	13	16	20	25
Density measured by density gradient column (average of two separate measurements) (ρ_{DGC})	0.9079	0.9219	0.9380	0.9415	0.9537	0.9708
Apparent crosslink density (mol $cm^{-3} \times 10^{-4}$) and standard deviation (calculated on three to six measurements)	2.26 0.10	8.04 0.43	17.55 0.37	19.90 0.80	26.46 0.64	40.98 0.67
Calculated density ($\rho_{calc.}$) $\rho_{NR} = 0.9080$ $\rho_{perox.} = 1.001$	0.9108	0.9154	0.9201	0.9229	0.9266	0.9313
CT numbers (H) and standard deviation	−137.7 1.3	−121.6 1.2		−111.2 1.4	−97.1 1.3	−83.2 1.4

Contribution due to curing

$$= \frac{0.0016145 - 0.0005342}{0.0016145} = 0.669 \quad (12)$$

i.e. 66.9% of the density increase is caused by the curing, a figure which compares well with the figure reported under Experiment I.

The linear regression equation for the contribution of the crosslinking to the density increase ($\rho_{crossl.}$) thus becomes

$$\rho_{crossl.} = 0.9080 + 0.0010803\,ACD \quad (13)$$

The CT numbers (H) for five of the six specimens, specially prepared for tomographic examination, were measured with a Siemens Somatom DR CT scanner at the Central Hospital in Boden, Sweden. Technical details of the CT scanner used can be found in reference 2.

The following machine settings were used:

X-ray tube voltage	125 kV
Dose	780 mAs
Slice thickness	2 mm
Scan time	7 s
Matrix size	512 × 512

The CT-numbers were averaged over an area of 60 × 8 mm.

The results obtained are shown in *Table 2*. The linear regression equation for apparent crosslink density (ACD) against CT number is:

$$ACD = 91.353 + 0.664\,CT(H) \quad (14)$$

$r = 0.985$.

All measured and calculated data have been plotted in *Figure 3*, where calculated and measured density and CT number are shown as a function of ACD. This graph facilitates assessment of the smallest density change caused by crosslinking which is likely to be detectable by a CT scanner. Combination of equations (13) and (14) gives:

$$\rho_{crossl.} = 0.9080 + 0.0010803 \times (91.353 + 0.664\,CT(H)) \quad (15)$$

If the CT number is changed by 1 Hounsfield unit (1 H), from say −100 to −101 H, $\rho_{crossl.}$ decreases by 0.717 mg cm^{-3}.

A tomographic image always contains some noise. Typical noise figures, quoted as standard deviations σ are shown in *Table 2*. The averaged σ values from *Table 2* yield 1.32 H and 3σ (99.5% confidence level) yields 3.96 H i.e. approximately 4 H and hence the smallest density variation which can be detected is approximately 4×0.72 mg $cm^{-3} = 2.88$ mg cm^{-3}. This result is in excellent agreement with data reported by Friddell *et al.*[3] who have suggested a lower detectable limit of 2–3 mg cm^{-3} for a normal medical X-ray CT scanner.

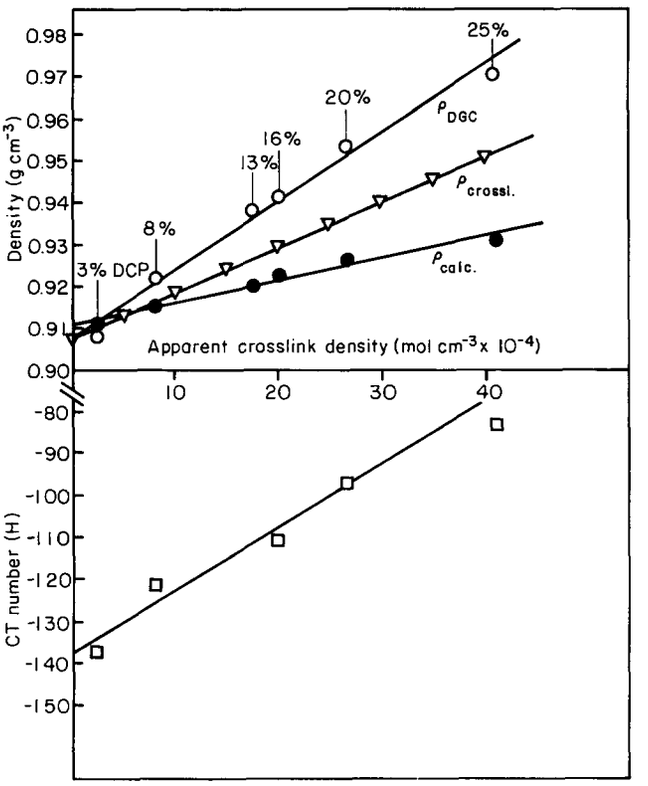

Figure 3 Density (using density gradient column, ρ_{DGC}, together with calculated density, $\rho_{calc.}$, and the contribution of crosslinking, $\rho_{crossl.}$, to the density increase) as a function of apparent crosslink density for DCP cured synthetic *cis*-1,4 polyisoprene. The lower part of the figure shows CT number (H) as a function of apparent crosslink density

ACKNOWLEDGEMENTS

I wish to thank Mr Erik Östman of the Industrial Development Center, Skellefteå, Sweden for making all the tomographic measurements.

Skega AB and the National Swedish Board for Technical Development (STU) are gratefully thanked for financial support.

REFERENCES

1 Persson, S. and Östman, E. *Polym. Test.* 1986, **6**, 407
2 Persson, S. and Östman, E. *Appl. Optics* 1985, **24**, 4095
3 Friddell, K. D., Lowrey, A. R., Lempiere, B. M. and Cruikshank, D. W. 'Topical Meeting on Industrial Applications of Computed Tomography and NMR-Imaging', paper MA3. Optical Society of America, 1984
4 McCullough, E. C. *Med. Phys.* 1975, **2**, 307
5 Keenleyside, G. F. Atomic Energy of Canada Ltd 1985, No. 2, 1
6 Zaty, L. M. in 'Radiology of the Skull and Brain. Technical Aspects of Computed Tomography' (Eds T. H. Newton and D. G. Potts), C. V. Mosley Company, St Louis, 1981
7 Brooks, R. A. and DiChiro, G. *Med. Phys.* 1976, **3**, 237
8 ASTM D279-81. 15.1.2 Hydrostatic Method
9 Tung, L. and Taylor, W. C. *J. Polym. Sci.* 1956, **21**, 144
10 Persson, S. *Polym. Test.* 1986, **6**, 47
11 Sheehan, C. J. and Bisio, A. L. *Rubb. Chem. Tech.* 1966, **39**, 149
12 Mason, P. *Polymer* 1964, **5**, 625